Radar Observations of TC Structures

Wen-Chau Lee NCAR/EOL

- Introduction
- Dual-Doppler radar methodology
- TC structures
- VTD and Operational aspects
- Summary

Introduction

- First airborne dual-Doppler observation in Hurricane Debby (1982) – Marks and Houze (1984)
- Ground-based Doppler observation in remain of Hurricane Alicia (1983) – Bluestein and Hazen (1989)
- First ground-based Doppler observation in Typhoon Vernon (1987) by the CAA radar

First Concept of Airborne Doppler Radar

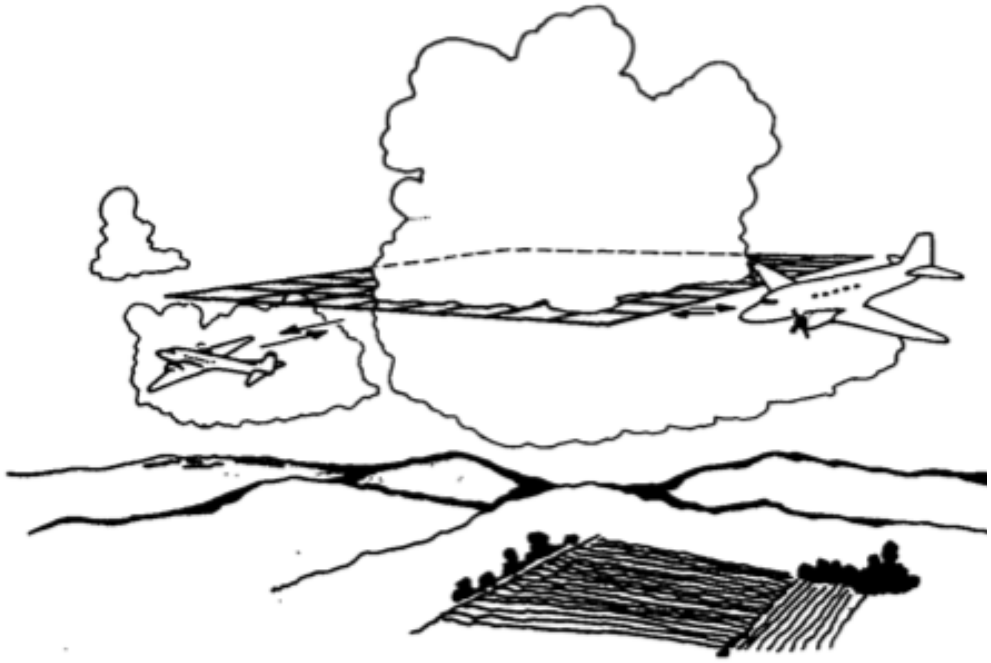

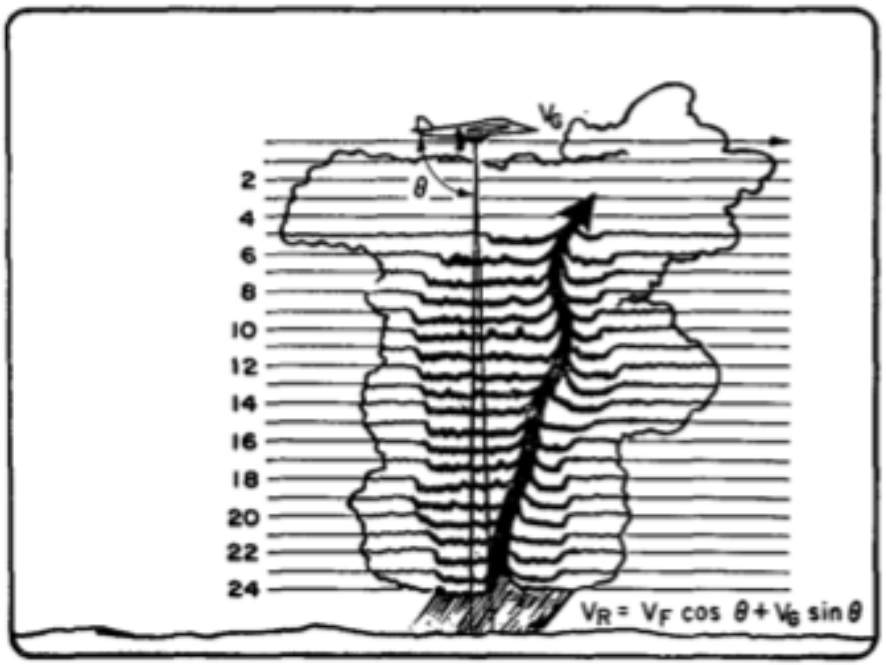

Lhermite (1971) – Journal of Applied Meteorology

Basic Dual-Doppler Analysis

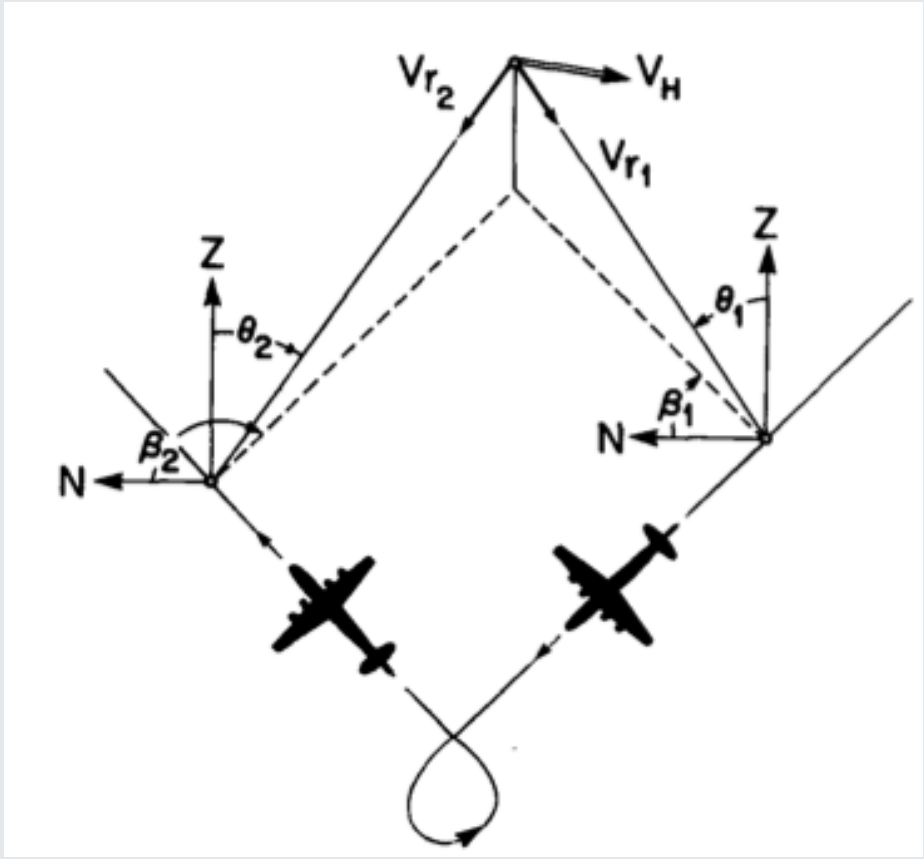

$$V_{r1} = U \sin\beta_1 \sin\theta_1 + V \cos\beta_1 \sin\theta_1 + (W + V_T + V_A) \cos\theta_1,$$

$$V_{r2} = U \sin\beta_2 \sin\theta_2 + V \cos\beta_2 \sin\theta_2 + (W + V_T + V_A) \cos\theta_2,$$

$$U = \frac{1}{\sin(\beta_1 - \beta_2)} \left[\frac{v_1 \cos\beta_2}{\sin\theta_1} - \frac{v_2 \cos\beta_2}{\sin\theta_2} \right],$$

$$V = \frac{1}{\sin(\beta_1 - \beta_2)} \left[\frac{v_2 \sin\beta_1}{\sin\theta_2} - \frac{v_1 \sin\beta_1}{\sin\theta_1} \right].$$

Jorgensen, Hildebrand, Frush (1983) – Journal of Applied Meteorology

Multi-Doppler Synthesis

$$V_r = u\sin(a)\cos(e) + v\cos(a)\cos(e) + (w + w_t)\sin(e)$$

$$\begin{pmatrix} \sin^2 a\cos^2 e & \sin a\cos a\cos^2 e & \sin a\cos e\sin e \\ \sin a\cos a\cos^2 e & \cos^2 a\cos^2 e & \cos a\cos e\sin e \\ \sin a\cos e\sin e & \cos a\cos e\sin e & \sin^2 e \end{pmatrix} \begin{pmatrix} u \\ v \\ w + w_t \end{pmatrix} = \begin{pmatrix} V_r \sin a\cos e \\ V_r \cos a\cos e \\ V_r \sin e \end{pmatrix}$$

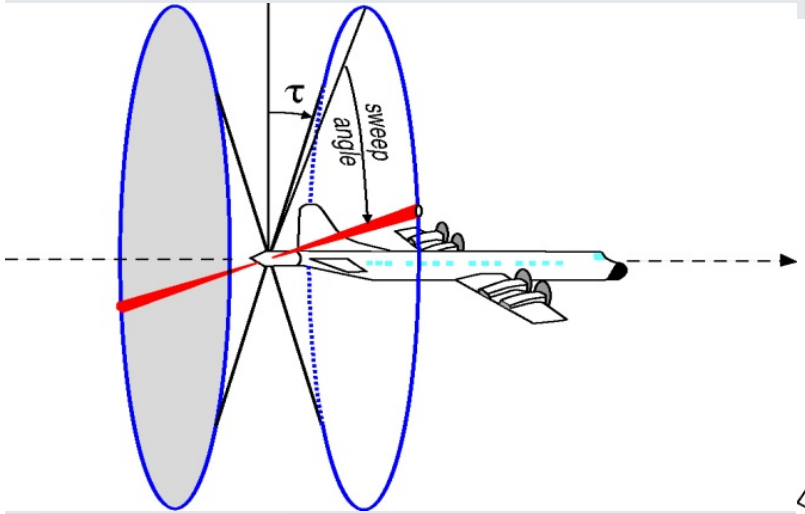

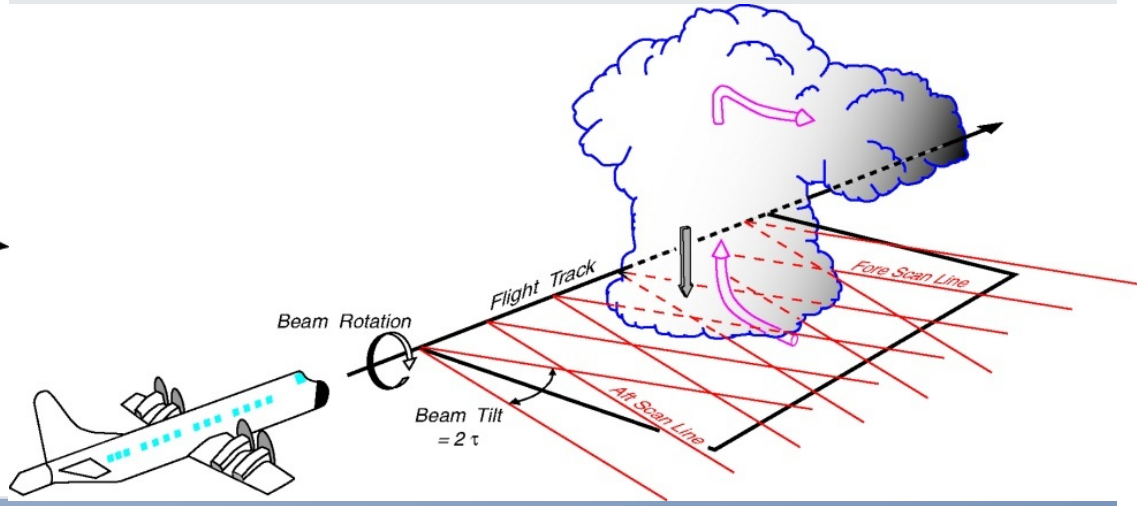

Hildebrand et al 1996

Doppler Synthesis Approaches

- **Forward Local** (Sprint/Reorder & Cedric)
  - Empirical Interpolation of V_r (Distance weighted averaging), then local synthesis
- **Forward Global** (Gamache, Raymond & Carrillo*)
  - Empirical Interpolation, then global synthesis
- **Reverse Global** (Gao et al. 1999/2004, Bell)
  - Interpolation from grid to radar space during cost function minimization

3-D Variational Formulation (Gamache 1997, Reasor et al 2009): Solve two or more radial velocity equations and mass continuity equation simultaneously.

$$F = \lambda_1 J_1 + \lambda_2 J_2 + \cdots + \lambda_n J_n + \lambda_{n+1} J_{n+1} + \lambda_{n+2} J_{n+2} + \lambda_{n+3} J_{n+3}$$

$$J_m = \sum_{l=1}^{L} \sum_{k=1}^{K} \sum_{j=1}^{J} \sum_{i=1}^{I} \rho_k (V_{rml} - u_{ijk} \cos\theta_{ml} \cos\phi_{ml} - v_{ijk} \sin\theta_{ml} \cos\phi_{ml} - w_{ijk} \sin\phi_{ml} - v_{Tml} \sin\phi_{ml})^2 \alpha_{ijkl}$$

$$J_{n+1} = \sum_{k=1}^{K} \sum_{j=1}^{J} \sum_{i=1}^{I} (\nabla \cdot \rho_k \vec{V}_{ijk})^2$$

$$J_{n+2} = \sum_{k=1}^{K} \sum_{j=1}^{J} \sum_{i=1}^{I} \left\{ \left(\frac{\partial^2 \rho u_{ijk}}{\partial x^2} \right)^2 + \left(\frac{\partial^2 \rho u_{ijk}}{\partial y^2} \right)^2 + \left(\frac{\partial^2 \rho u_{ijk}}{\partial z^2} \right)^2 + \left(\frac{\partial^2 \rho v_{ijk}}{\partial x^2} \right)^2 + \left(\frac{\partial^2 \rho v_{ijk}}{\partial y^2} \right)^2 + \left(\frac{\partial^2 \rho v_{ijk}}{\partial z^2} \right)^2 \right.$$
$$+ \left(\frac{\partial^2 \rho w_{ijk}}{\partial x^2} \right)^2 + \left(\frac{\partial^2 \rho w_{ijk}}{\partial y^2} \right)^2 + \left(\frac{\partial^2 \rho w_{ijk}}{\partial z^2} \right)^2 + \left(\frac{\partial^2 \rho u_{ijk}}{\partial x \partial y} \right)^2 + \left(\frac{\partial^2 \rho u_{ijk}}{\partial x \partial z} \right)^2 + \left(\frac{\partial^2 \rho v_{ijk}}{\partial y \partial z} \right)^2$$
$$\left. + \left(\frac{\partial^2 \rho v_{ijk}}{\partial x \partial y} \right)^2 + \left(\frac{\partial^2 \rho v_{ijk}}{\partial x \partial z} \right)^2 + \left(\frac{\partial^2 \rho v_{ijk}}{\partial y \partial z} \right)^2 + \left(\frac{\partial^2 \rho w_{ijk}}{\partial x \partial y} \right)^2 + \left(\frac{\partial^2 \rho w_{ijk}}{\partial x \partial z} \right)^2 + \left(\frac{\partial^2 \rho w_{ijk}}{\partial y \partial z} \right)^2 \right\}$$

$$J_{n+3} = \sum_{k=1}^{K} \sum_{j=1}^{J} \sum_{i=1}^{I} \rho_k (w_{ijk} - w_B)^2 \delta_B$$

Advantages / Disadvantages

	Error Propagation	Memory/ CPU	Diagnostics	Multiple Data Sources	Anisotropic Filtering	Extra Balance Constraints
Forward Local	Vertical	Low/Fast	Established	Difficult	Possible	Difficult
Forward Global	Horizontal & Vertical	High/ Slow	Complex	Possible	Difficult	Possible
Reverse Global (Bell)	BG Error Covariance	Low/Slow	Moderate	Yes	Yes	Possible

Multiple analysis techniques are a good thing!

Navigation Correction

- Drift
- Pitch
- Roll
- Aircraft H. Speed
- Aircraft V. Speed
- Aircraft Altitude
- Tilt (Fore)
- Tilt (Aft)

Testud et al. (1995)
Georgis et al. (2000)
Bosart et al. (2002)

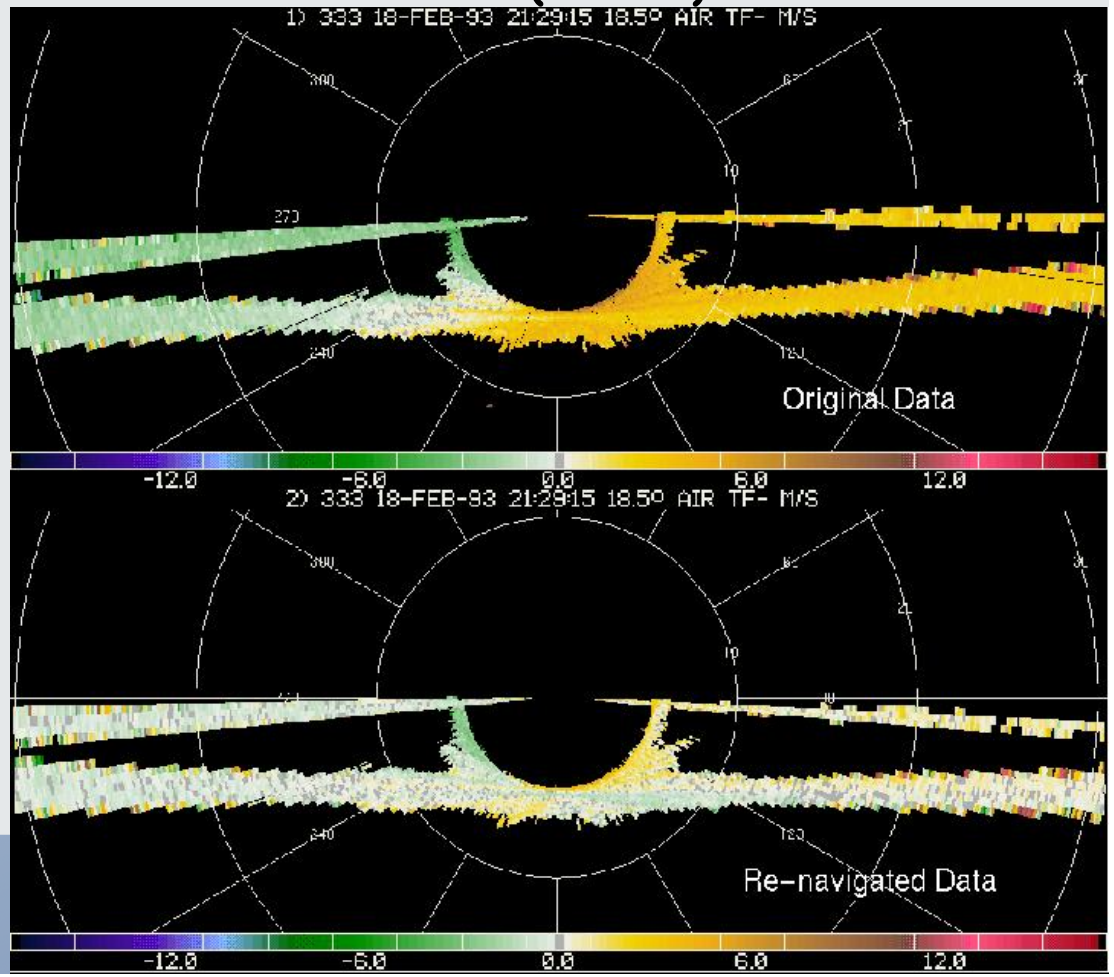

Data QC (A Nightmare)

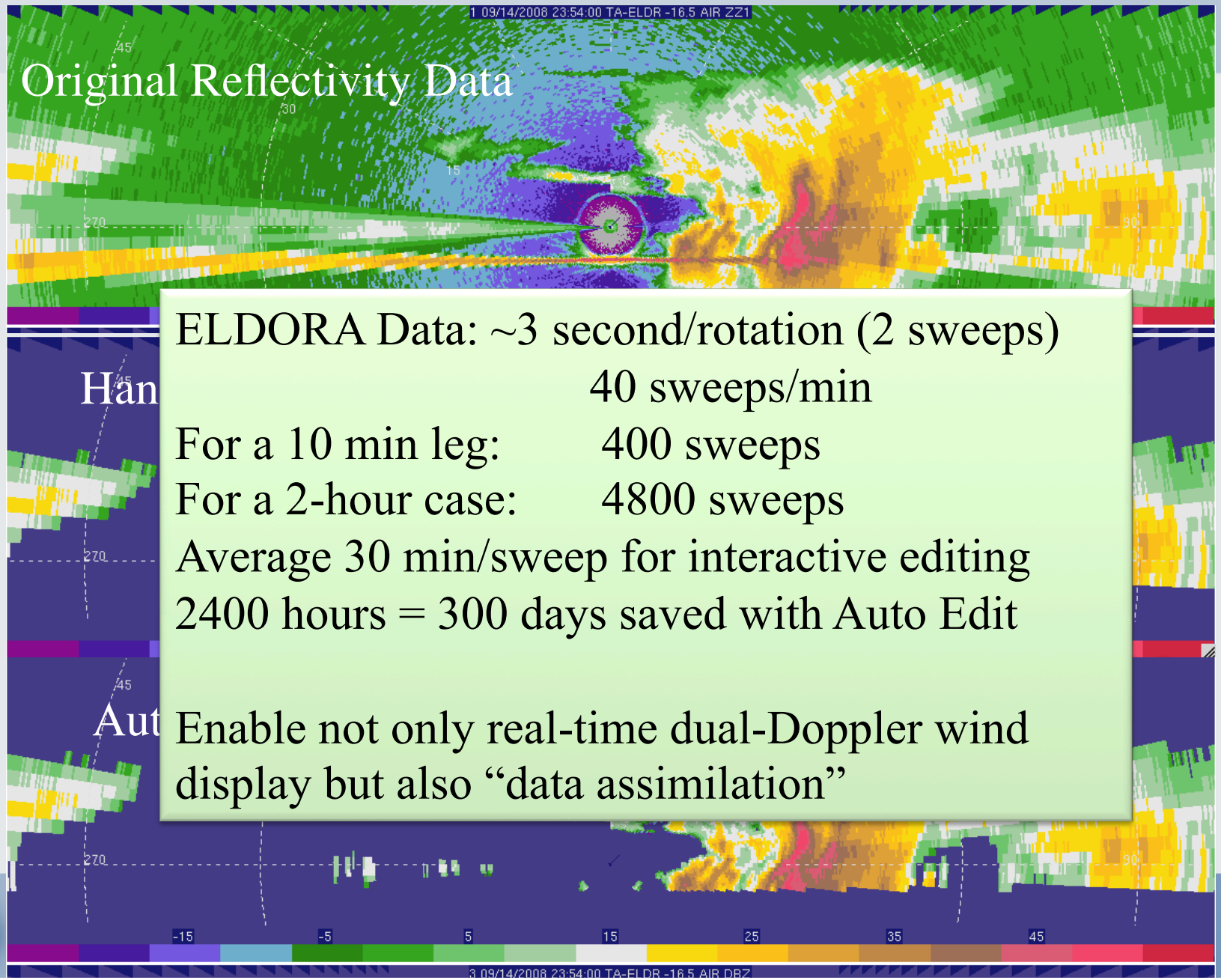

ELDORA Data: ~3 second/rotation (2 sweeps)
40 sweeps/min

For a 10 min leg: 400 sweeps

For a 2-hour case: 4800 sweeps

Average 30 min/sweep for interactive editing

2400 hours = 300 days saved with Auto Edit

Enable not only real-time dual-Doppler wind display but also “data assimilation”

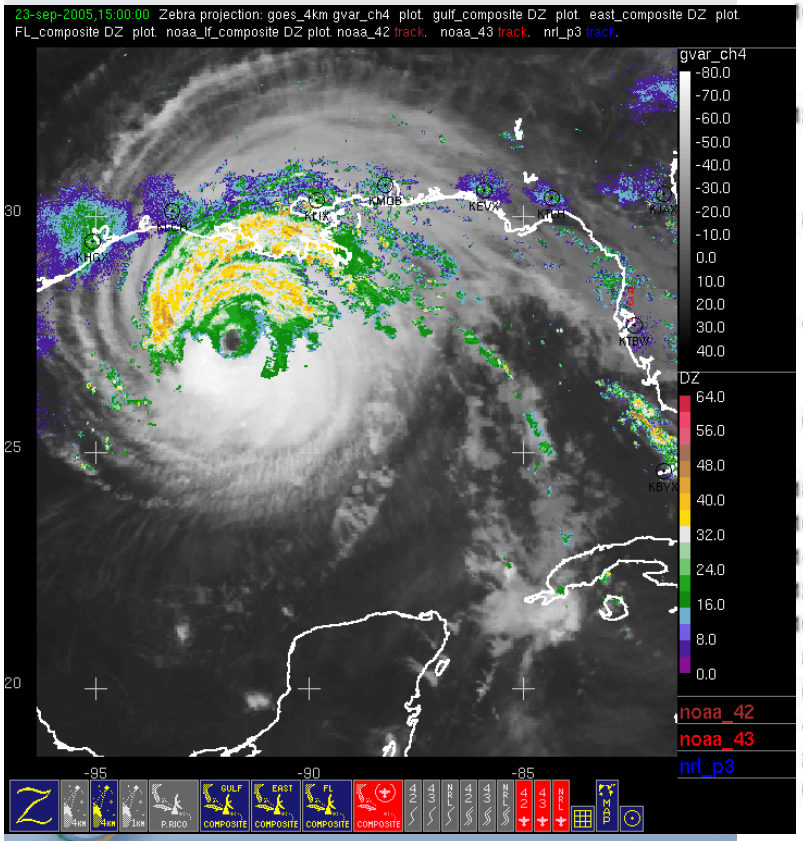
23-sep-2005,15:00:00 Zebra projection: goes_4km gvar_ch4 plot. gulf_composite DZ plot. east_composite DZ plot.
FL_composite DZ plot. noaa_lf_composite DZ plot. noaa_42 track. noaa_43 track. nrl_p3 track.
gvar_ch4
-80.0
-70.0
-60.0
-50.0
-40.0
-30.0
-20.0
-10.0
0.0
10.0
20.0
30.0
40.0
DZ
64.0
56.0
48.0
40.0
32.0
24.0
16.0
8.0
0.0
noaa_42
noaa_43
nrl_p3
KTLH
KEVX
KTBW
KBYX
30
25
20
-95
-90
-85

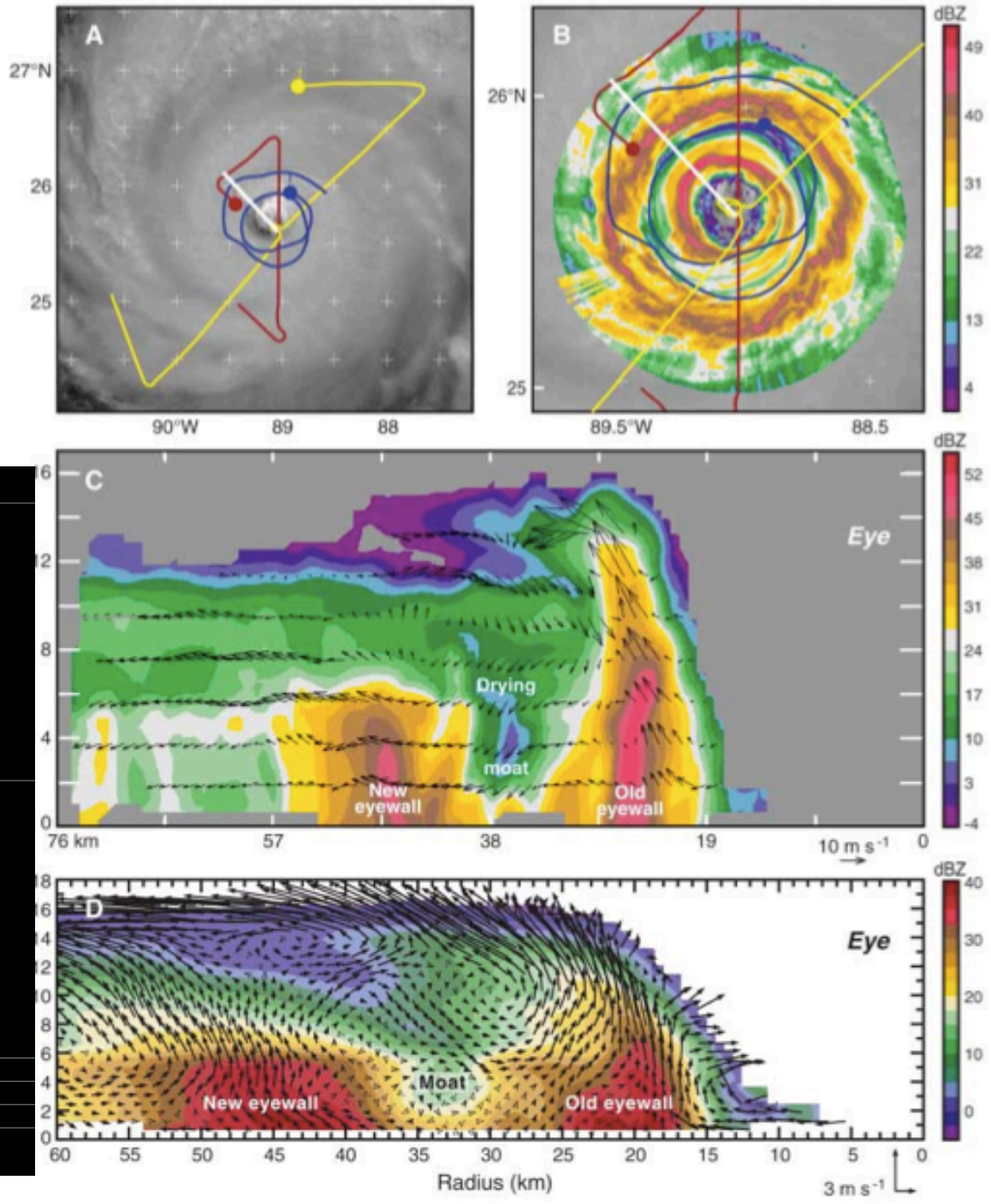
A
27°N
26
25
90°W
89
88
B
26°N
25
89.5°W
88.5
dBZ
49
40
31
22
13
4
C
Eye
Drying
moat
New eyewall
Old eyewall
76 km
57
38
19
0
10 m s-1
dBZ
52
45
38
31
24
17
10
3
-4
D
Eye
New eyewall
Moat
Old eyewall
60
55
50
45
40
35
30
25
20
15
10
5
0
Radius (km)
3 m s-1
dBZ
40
30
20
10
0

Rainband Structures

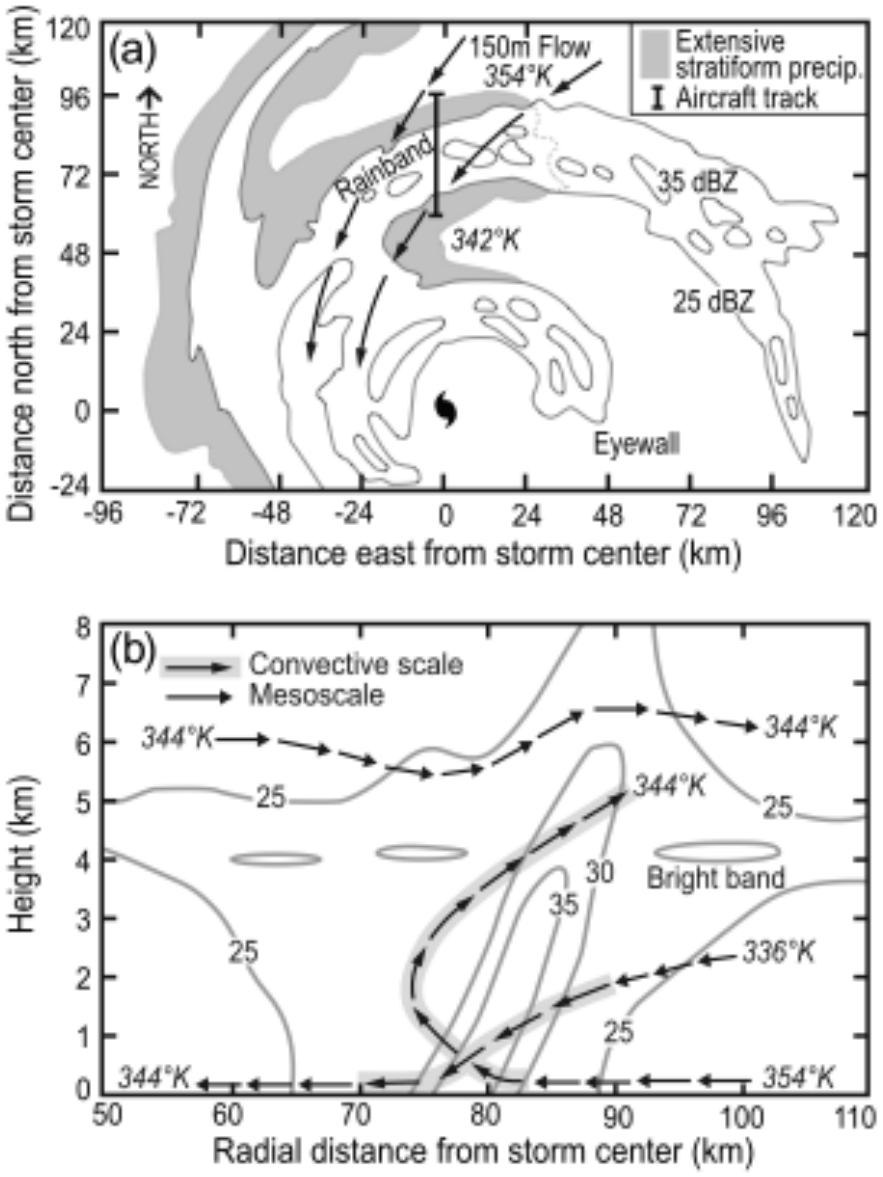

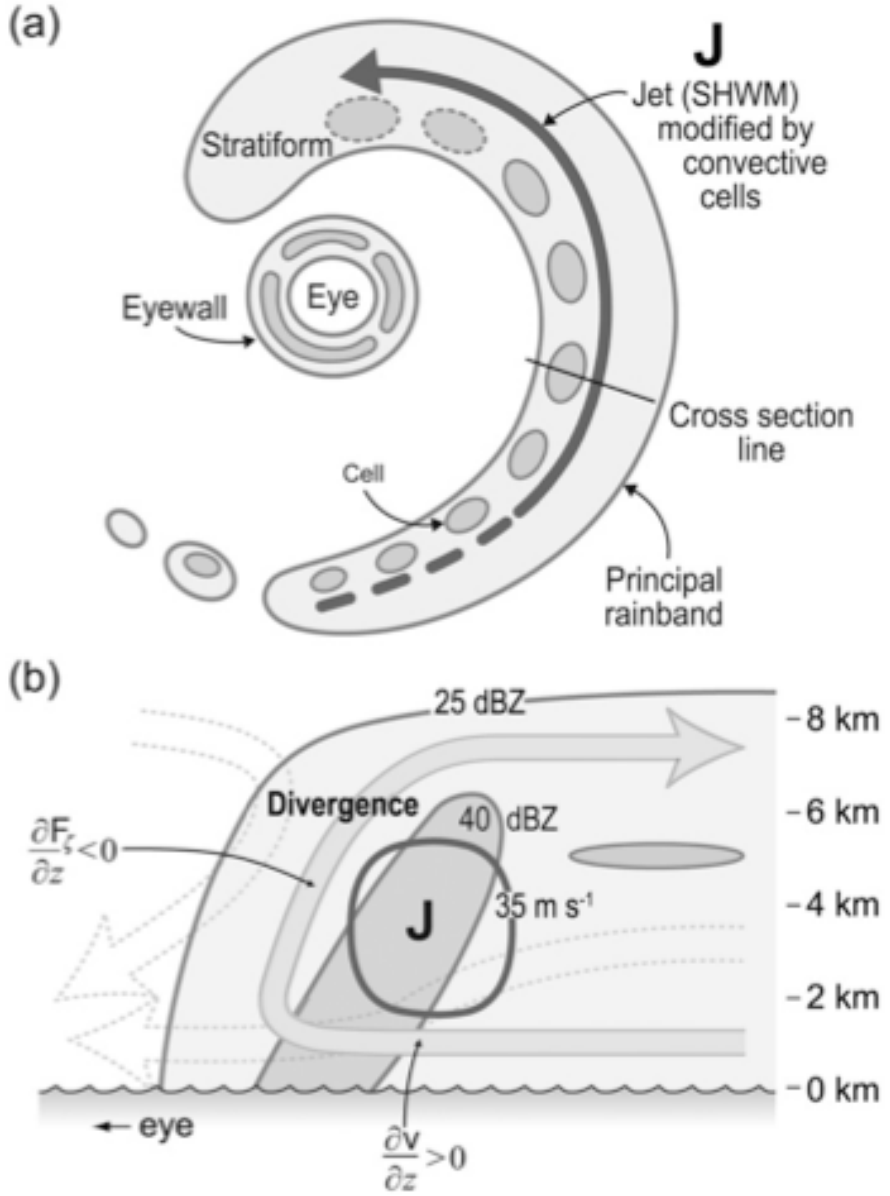

Miniature Supercells in TC Rainbands

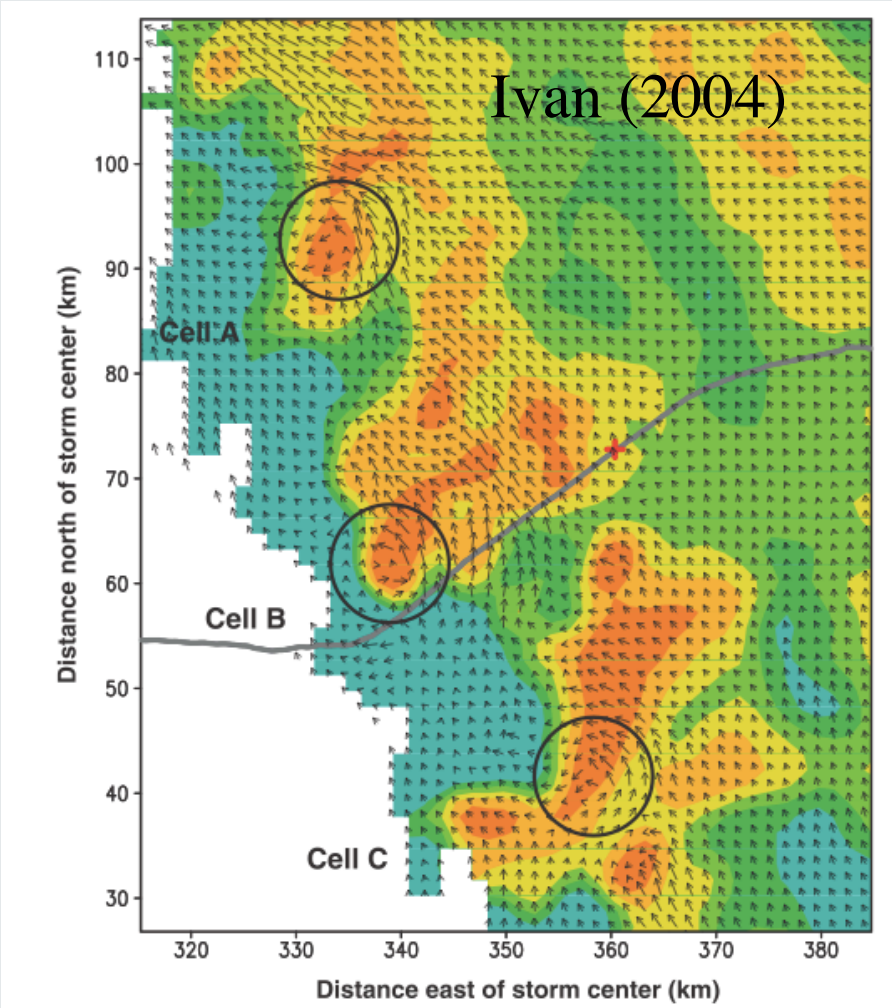

Eastin and Link (2009)

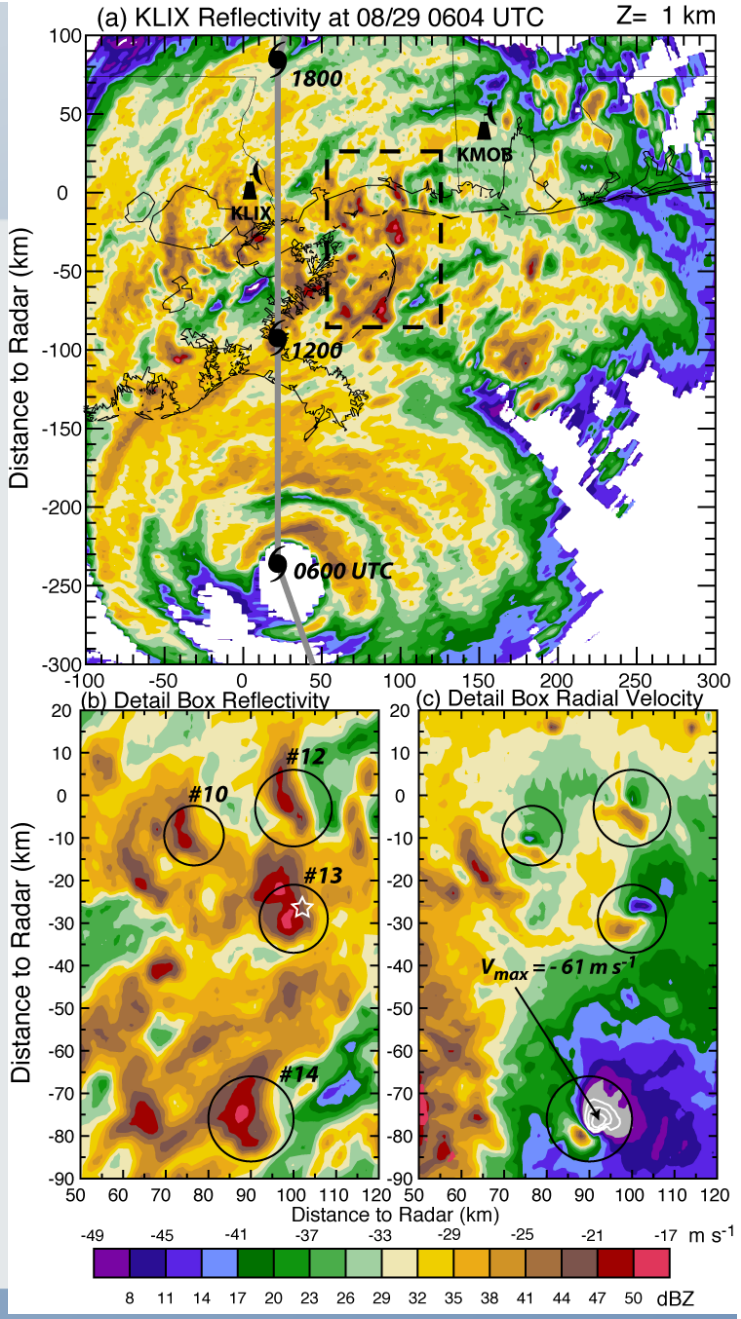

Lee et al. (2008)

Investigate Tropical Cyclone Genesis Using ELDORA Data
Robert Houze, Wen-Chau Lee, Michael Bell (2009)

Unprecedented 300 m resolution of a convective burst episode during RAINEX (2005)

Where is potential vorticity generated during TC genesis?

Supports the bottom up theory, one of the two competing TC genesis theories.

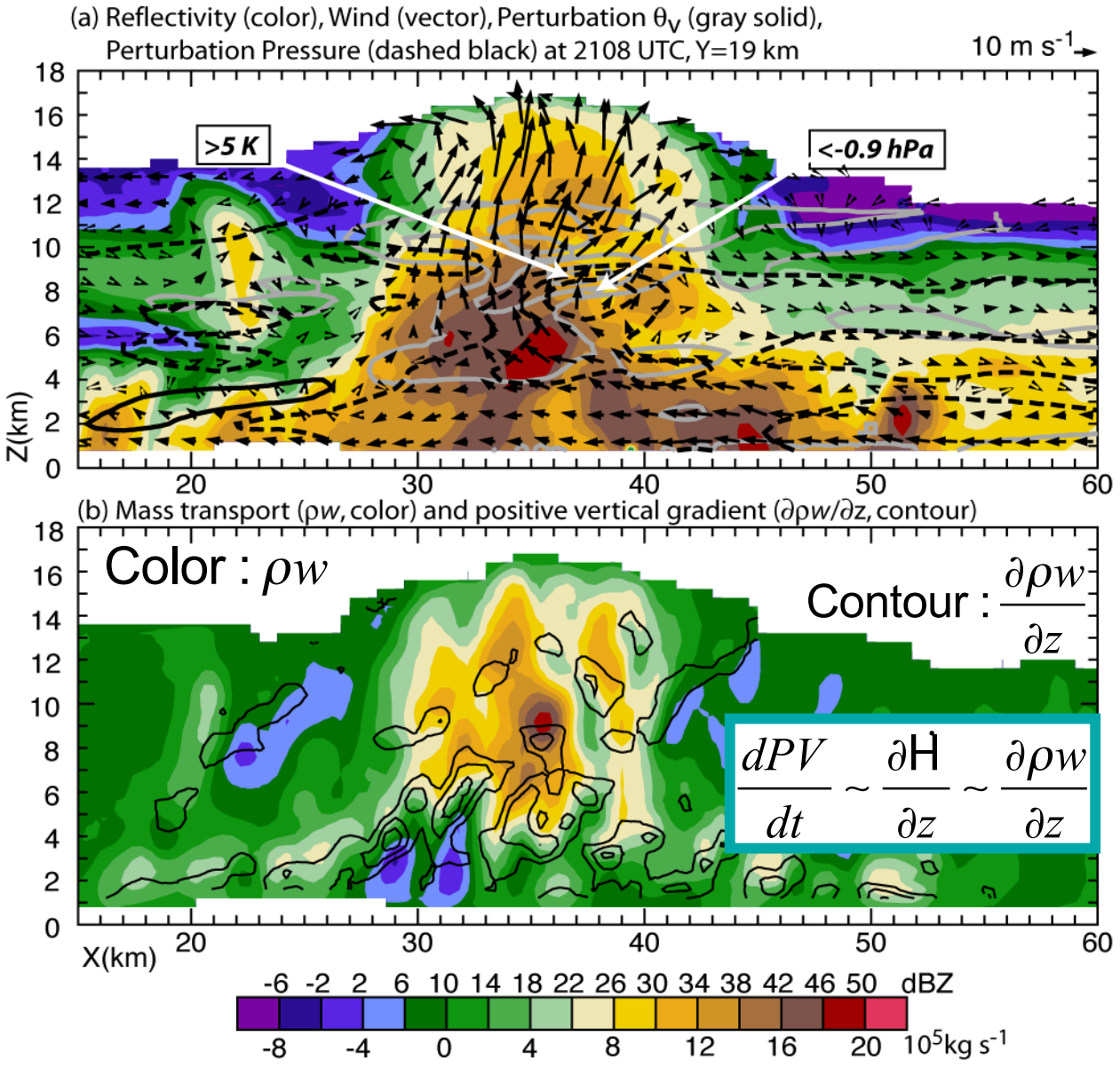

Velocity Track Display (VTD)

Velocity Track Display (VTD)
31 August 1988

1. General Concepts

This is just to put down some elementary concepts for real-time data interpretation from a single beam airborne Doppler radar scanning (nominally) in a track-orthogonal plane. The ideas are mostly borrowed from established techniques with ground-based radars for interpretation of convective scale phenomena such as gust fronts, mesocyclones and tornadoes, microbursts, etc. The radar itself only measures one component of horizontal flow when the flight track is a straight line segment. This is unlike ground-based radars which scan about a vertical axis (PPIs) and thereby measure different components of horizontal flow surrounding the radar. The harmonic content of such data permits direct computation of horizontal divergence, mean flow and deformation as long as the flow roughly satisfies linearity and stationarity assumptions.

The basic difference between airborne and ground-based MESOSCALE kinematic analyses is in mobility of the platform such that a single comp nent measured is observed "everywhere" in the domain. A ground-based rad measures both horizontal components, each in separate parts of the domain Unlike ground-based harmonic analyses, certain airborne analyses are not constrained either to linearity or to irrotational assumptions. example, relative vorticity may be inferred from periodic behavior of one horizontal velocity component along the track.

There is no fundamental difference between airborne and ground-ba Doppler measurements of CONVECTIVE scale circulations. Ground-based Dopp observations are typically made at ranges of several tens of kilometers c Convective scale features such as updrafts, downdrafts, mesocyclones, tor and microbursts are several kilometers or less in horizontal extent. Thi aspect ratio (between radar range and horizontal scale of convective circulations) means that individual convective circulations subtend a sma azimuth sector. Most techniques for qualitative and quantitative evaluat assume parallel beams - a condition more rigorously satisfied in the case airborne Doppler. These techniques may be applied directly to studies of convective cores - including detailed convective line inflow, outflow and and shallow, PBL-dominated, rainband and eyewall propagation studies. Furthermore, with the added assumption of stationarity, the same ground-b convective-scale techniques apply to larger scale phenomena such as the primary hurricane core circulation.

Owing to the horizontal scan axis of airborne Doppler data and to platform mobility, it is particularly straightforward to take advantage of slab-symmetric and axi-symmetric circulation models where flight paths are parallel to rainbands, squall lines and eyewalls. While only one horizontal component is observed, that component may be selected on the basis of slab- or axi-symmetry thereby capturing first order derivative fields associated with the transverse circulations. The horizontal scan axis also permits strong inference of vertical transport of horizontal momentum in updrafts and downdrafts within the scan plane. This may be extended to near-real-time averaging along flight tracks parallel to bands and eyewalls with vertical integration of the 2-D continuity equation. This yields the position of updrafts and downdrafts in relation to cores of precipitation, the shear of their

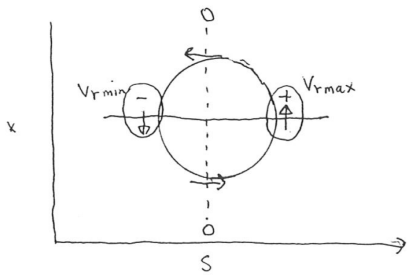

Fig 9a non-divergent, symmetric

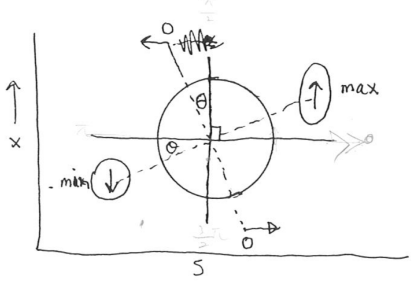

Fig 9c divergent / symmetric

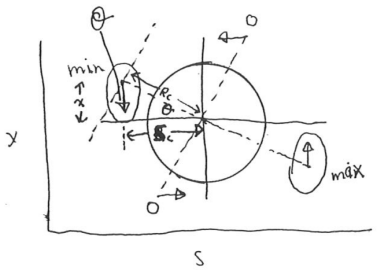

Fig 9b convergent/symmetric

Fig 10 – NEXT PAGE

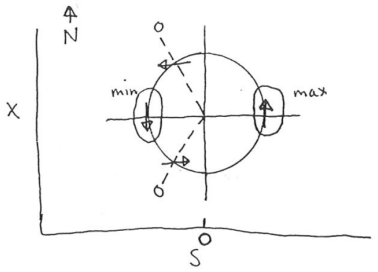

Fig 9d. divergent north
convergent south
non-div east & west

The Grand Parents of VTD – Carbone and Marks (1989)

3C.1

VELOCITY TRACK DISPLAY (VTD): A REAL-TIME APPLICATION FOR AIRBORNE DOPPLER RADAR DATA IN HURRICANES

R. E. Carbone
National Center for Atmospheric Research*
Boulder, Colorado 80307

Frank D. Marks, Jr.
Hurricane Research Division, NOAA/AOML
Miami, FL 33149

1. INTRODUCTION

The Hurricane Research Division of NOAA will transmit real-time airborne Doppler analyses of hurricane wind fields during reconnaissance flights for use at the National Hurricane Center. This paper outlines some elementary concepts for these data analyses from a single-beam airborne Doppler radar. We assume that the radar is scanning in a track-orthogonal plane and that the aircraft track is a radial penetration toward (and from) the hurricane's circulation center.. For the most part, these ideas represent adaptations of established techniques with ground-based radars.

A quarter century ago, Atlas (1963) and Lhermitte (1964) discussed basic concepts associated with Doppler radar observations including hurricane and tornado vortex circulations. Browning and Wexler (1968) extended and quantified the so-called "VAD" technique developed by Caton (1963) for ground-based radars. The VAD technique allows estimation of mean horizontal divergence, mean wind and deformation of flow from data typically acquired on a scale of several tens of kilometers in conical (PPI) scan. Smaller, convective-scale vortices, may be quantified by means of radial and azimuthal shear patterns as demonstrated by Zrnic and Doviak (1975), Burgess (1976), Brown et al. (1978). Baynton (1979) applied a similar approach specifically to the hurricane problem. These techniques are described together with examples of Doppler velocity fields measured in ELENA and GLORIA from the NOAA P-3 aircraft as shown in Figs. 1 and 2, respectively.

2. DOPPLER VELOCITY AND TANGENTIAL WIND-SPEED

An important aspect of the hurricane wind field that can be derived in real-time from airborne Doppler data is the hurricane's tangential circulation speed, V_T, as a function of radius from the storm center, R, and height, z. At present, only in situ data are used for determination of V_T at one altitude (e.g. Willoughby, 1984, 1989) where variation of V_T with R is derived from a time-to-space conversion. The vertical scanning capability of Doppler radar allows the extension of this approach to include the variation of V_T with z as well as R. A single sweep of the radar provides a 2-D velocity field in a quasi-vertical plane orthogonal to the flight track. When the aircraft track approximates a storm-radial penetration and the flow is quasi-circular, then the Doppler velocity field, V_r, is a relatively simple function of $V_T(R,z)$ and pointing angle:

$$V_T(R,z) = V_r(r,\theta)/\sin(\theta)\cos(\phi) \qquad (1)$$

where $\phi = \sin^{-1}(r\cos\theta/R)$; theta is the "elevation" angle in ground-based radar parlance (but hereinafter referred to as "azimuth") with 0 deg at zenith and 180°at nadir; ϕ is the angle subtended by the flight track and a radius vector from the storm center to the pulse volume (r, θ). When r/R is of order 0.2 or less, then dependence on ϕ vanishes for practical applications herein. In (1) we have omitted the terms associated with vertical airspeed and hydrometeor fallspeed which tend to be much less than 0.1 V_T for low-pass filtered data and for the values of θ actually used in V_T computation. Dependence on θ vanishes at flight-level.

3. VORTEX FEATURES NEAR FLIGHT LEVEL

Observation of any vortex with a sequence of parallel (or quasi-parallel) radar beams reveals a pattern of beam-to-beam shear usually described as a vortex couplet. In the case of airborne radar flying a radial penetration, the cross-track windshear pattern is as shown in Fig. 1a. This is entirely analogous to azimuthal shear for small vortices observed from a relatively long distance by ground-based radars in PPI scan.

Following the analysis of Burgess (1976), Figs. 3 illustrate, schematically, the family of isodop patterns which result from a radial vortex penetration. Fig. 3a shows the V_{Tmax}, V_{Tmin} and V_T=0 isodops for a symmetric, non-divergent vortex. Note that the max and min isodops are centered on the flight track, indicating flow orthogonal to the track. Also, the zero isodop passes through the circulation center and extends radially outward, orthogonal to the track. This is indicative of an axi-symmetric flow which is purely tangential with respect to the storm center.

Fig. 3b shows a symmetric and radially-inward flow superimposed on the tangential circulation. For obvious reasons, the V_{Tmax}, V_{Tmin} and V_T=0 isodops are rotated clockwise by the inflow angle, α, as a consequence of the hurricane-radial component of flow, V_R. Counter-clockwise rotation of the isodop pattern is caused by outward V_R. The expected pattern is similar to mesocyclone observations in supercell thunderstorms as described by Donaldson (1970) and Burgess (1976) among others. The sense of radial flow is a strong indication of horizontal divergence. Quadrant-averaged divergence may be estimated from the Doppler data in real time where V_R=V_{Tmax} sin α and DIV=2V_R/R assuming the primary circulation is circular.

Fig. 3c schematically illustrates the along-track V_T pattern with uniform tangential flow when there is radial outflow to the "north" and radial inflow to the "south" of the flight track. In this case, the V_{Tmax} and V_{Tmin} isodops may be located near the flight track but the V_T=0 isodop forms a right-pointing "V" pattern. This pattern is evident in data from ELENA shown in Fig. 1a where the flow contains a radially-inward component in three of the four storm quadrants.

From illustrations in Fig. 3, it is evident that mesoscale features of the vortex may be estimated in real-time as simple functions of α on the scale of storm quadrants utilizing by the Doppler velocity maxima, minima and zero-isodop lines. A more robust estimate may be achieved through adaptation of the VAD method after Browning and Wexler (1968). Following time/space conversion along the track, one may perform least squares, harmonic-decomposition fits to annuli of data about the circulation center in horizonal planes. A purely non-divergent, axi-symmetric circulation will constitute a perfect fit to the first harmonic. An axi-symmetric and divergent circulation will introduce a zeroth harmonic term. Radial flow asymmetries will introduce higher harmonics which are, intrinsically, deformative.

It should be noted that in-situ aircraft winds in the along-track direction may be combined with Doppler track-orthogonal winds (measured on both sides of the aircraft) to yield a continuous, and direct measure of horizontal divergence near flight level along the track. This may be performed at scales from a few km to 100 km, thus providing statistics on convective-scale and mesoscale circulation amplitudes.

4. V_T PROFILES

As noted earlier, airborne Doppler radar affords the potential to estimate V_T for all R and z. This requires processing of selected data from 360°"RHI" scans for all altitudes. A typical radar scan is shown in Fig. 2 where V_r is illustrated by gray-shade isodops. For θ substantially removed from zenith (or nadir) - say, $\pm 60°$– V_T may be approximated by half the difference of $V_r(r,\pm\theta)$ at two points symmetrically located about zenith (or nadir). This is analogous to four-beam UHF/VHF wind profiler techniques. It is also equivalent to averaging the upwind and downwind speed in a "VAD" analysis on a vertical plane similar to the method of Browning and Wexler (1968). For very small r, a complete "VAD" analysis may be performed for flight-level V_T estimation. A variation of harmonic analysis may be applied at constant altitude illustrated by the dashed line at 8km in Fig. 2. Application of (1) to $V_r(r,\theta)$ data at 8 km will yield numerous estimates of V_T(8km, θ, ϕ) for any given storm radius, R. The ensemble average $\langle V_T(R)\rangle$ may then be low-pass filtered in the time domain (R) and should generally provide an estimate of V_T superior to the simple two-point "profiler" method.

It can also be demonstrated that hydrometeor vertical velocity (w + V_f) is a first harmonic in quadrature-phase with respect to V_T. Given an applicable dBZ-V_f relationship, is possible to estimate mean vertical airspeed, w. The quality of V_T and w estimates is dependent upon the linearity of the wind field. If the wind field properties are similar to those normally associated with stratiform rain, then the estimates from harmonic analysis should be good. One measure of estimate uncertainties is the RMS residual from the harmonic fit. Performing these analyses for each sweep during a radial penetration of a hurricane yields an estimate of V_T and w at all storm radii and at all altitudes.

* The National Center for Atmospheric Research is sponsored by the National Science Foundation.

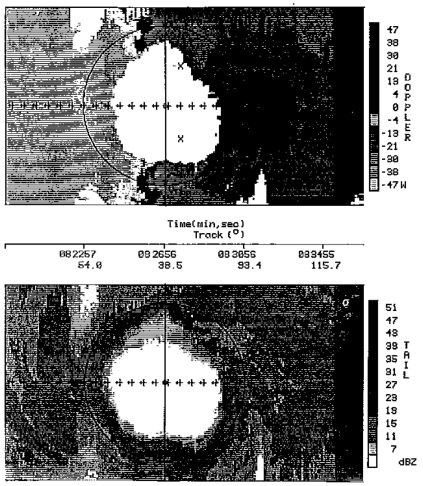

Fig. 1. VTD display of V_r (top) and reflectivity (bottom) at flight level (~3.0 km) from Hurricane Elena 2 September 1985. The gray shades indicate isodops of V_r (m s^{-1}) and reflectivity (dBZ). The V_r data have been unfolded, and V_r has been multiplied by sinθ. Hence, the velocities are either toward θ =270°(top of the image, -X), or toward θ=90°(bottom of the image, +X). The domain of the image is from -38 to 38 km in X (ordinate) and ~26. min in time (abscissa). The aircraft track is denoted by the small aircraft symbols.

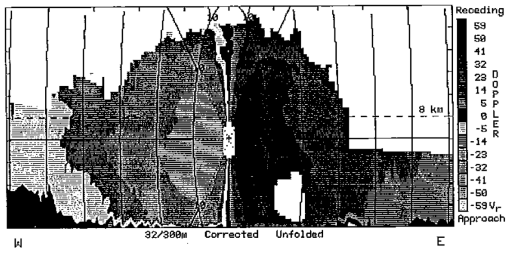

Fig. 2. (a) Single sweep of the airborne Doppler radar for 25 September 1985, in Hurricane Gloria. The gray shades indicate unfolded isodops of V_r (m s^{-1}). The domain of the image is from -60 to 60 km in X and 0-16 km in altitude. The aircraft position is denoted by the small "+" in the center of the image (radar altitude of 6.44 km) and the range rings are at 10 km intervals.

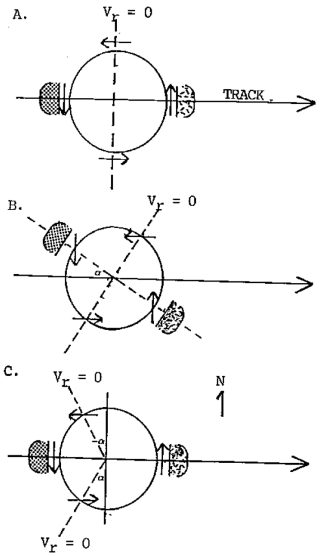

Fig. 3. Schematic representations of isodop maximum (dark), minimum (light) and V_r=0 (dashed) relative to aircraft flight track as in Fig. 1. (a) symmetric non-divergent (b) symmetric convergent (c) asymmetric with divergence "north" and convergence "south".

References

Atlas, D., 1963: Atmospheric Sciences: Visions versus mirages with regard to radar meteorology. *Bull. Amer. Meteor. Soc.*, 44, 772-777.

Baynton, H.W., 1979: The case for Doppler radars along our hurricane affected coasts. *Bull. Amer. Meteor. Soc.*, 60, 1014-1023.

Brown, R.A., L.R. Lemon, and D.W. Burgess, 1978: Tornado detection by pulsed Doppler radar. *Mon. Wea. Rev.*, 106, 29-38.

Browning, K.A., and R. Wexler, 1968: The determination of kinematic properties of a wind field using Doppler radar. *J. Appl. Meteor.*, 7, 105-113.

Burgess, D.W., 1976: Single Doppler radar vortex recognition: Part I: Mesocyclone signature. Preprints, *17th Radar Meteorology Conference*, , Amer. Meteor. Soc., Boston, 97-103.

Caton, P.A.F., 1963: Wind measurement by Doppler radar. *Meteorol. Mag.* 92, 213-222.

Donaldson, R.J., Jr., 1970: Vortex signature recognition by a Doppler radar. *J. Appl. Meteor.*, 9, 661-670.

Lhermitte, R.M, 1964: Doppler radars as severe storm sensors: *Bull. Amer. Meteor. Soc.*, 45, 587- 596.

Willoughby, H.E., F.D. Marks, Jr., and R.J. Feinberg, 1984: Stationary and propagating convective bands in asymmetric hurricanes. *J. Atmos. Sci.*, 41, 3189-3211.

Willoughby, H.E., 1989: Temporal changes of the primary circulation in tropical cyclones. submitted to *J. Atmos. Sci.*

Zrnic, D.S. and R.J. Doviak, 1975: Velocity spectra of vorticies scanned with a pulse-Doppler radar. *J. Appl. Meteor.*, 14, 1531-1539.

The VTD Family of Techniques

VTD – Lee et al. (1994)
EVTD – Roux and Marks (1996)
GBVTD – Lee et al. (1999)
GB-EVTD – Roux et al. (2004)
EGBVTD – Liou et al. (2006)
GVTD – Jou et al. (2008)
GrVTD – Wang et al. (near submission)

VTD Formulation

Axisymmetric Tangential Wind

Axisymmetric Radial Wind

For L=3, M=N=2:

$$V_M \cos(\theta_T - \theta_M) = (A_0 - A_2)/\cos\alpha_{\max}$$

$$V_T C_0 = -B_1 - B_3 - V_M \sin(\theta_T - \theta_M)\sin\alpha_{\max} - V_R S_2$$

$$V_R C_0 = A_1 + A_3 - V_R C_2$$

$$V_T S_1 = A_2 + A_0 - V_M \cos(\theta_T - \theta_M) - V_R C_1$$

$$V_T C_1 = -2B_2 + V_R S_1$$

$$V_T S_2 = 2A_3 - V_R C_2$$

$$V_T C_2 = -2B_3 + V_R S_2$$

VTD-derived Axisymmetric Quantities:

$$w = -\frac{1}{\rho}\int_{z=0}^{z=H} \rho\left(\frac{\partial V_R}{\partial R} + \frac{V_R}{R}\right)dz$$

Vertical Velocity

$$M = V_T R + \frac{1}{2} f R^2$$

Angular Momentum

$$\frac{\partial p}{\partial r} = -\rho\left(V_R \frac{\partial V_R}{\partial z} + w\frac{\partial V_R}{\partial z} - \frac{V_T^2}{R} - f V_T\right)$$

Pressure Gradient

Hurricane Charley Axisymmetric Structure 13/08 – 14/02 UTC

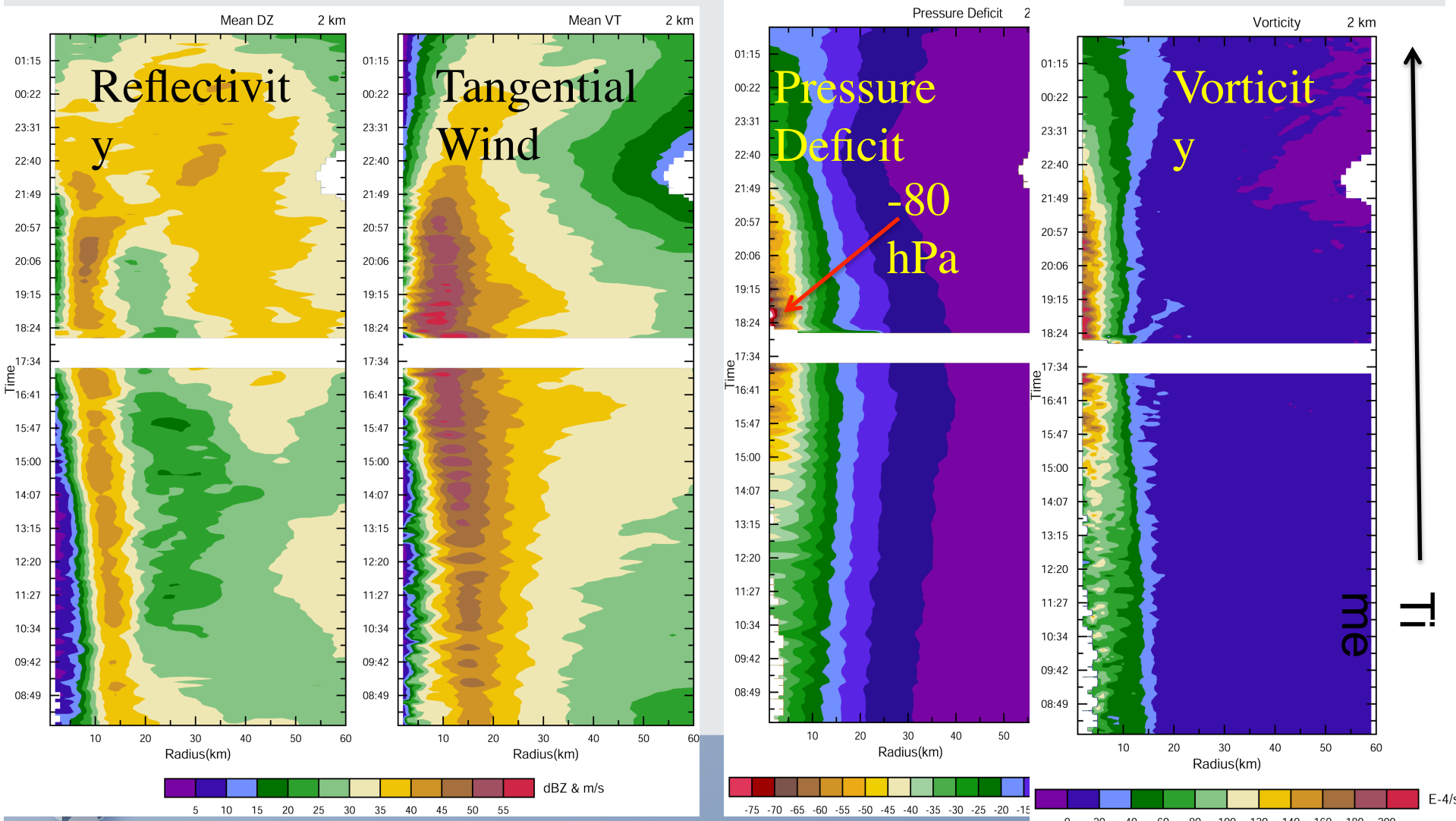

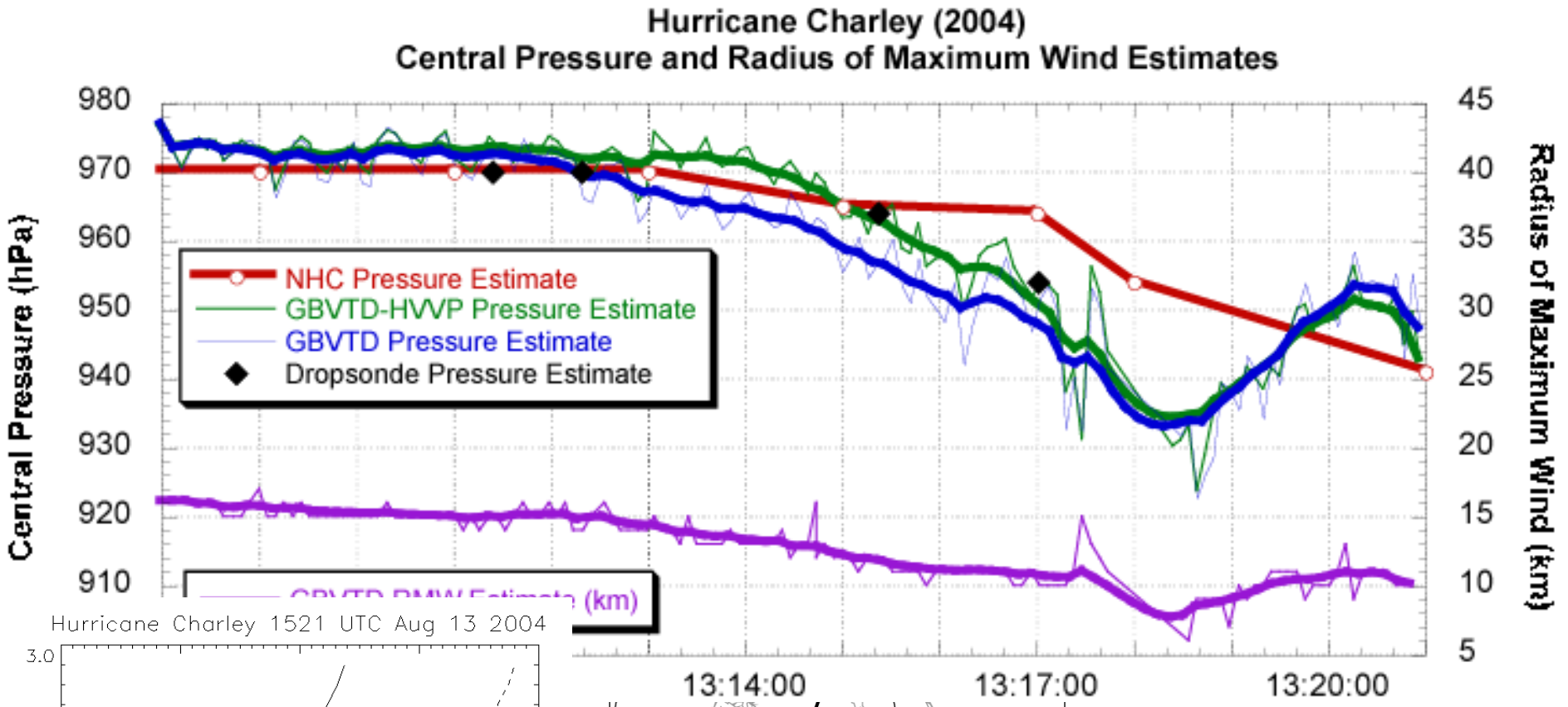

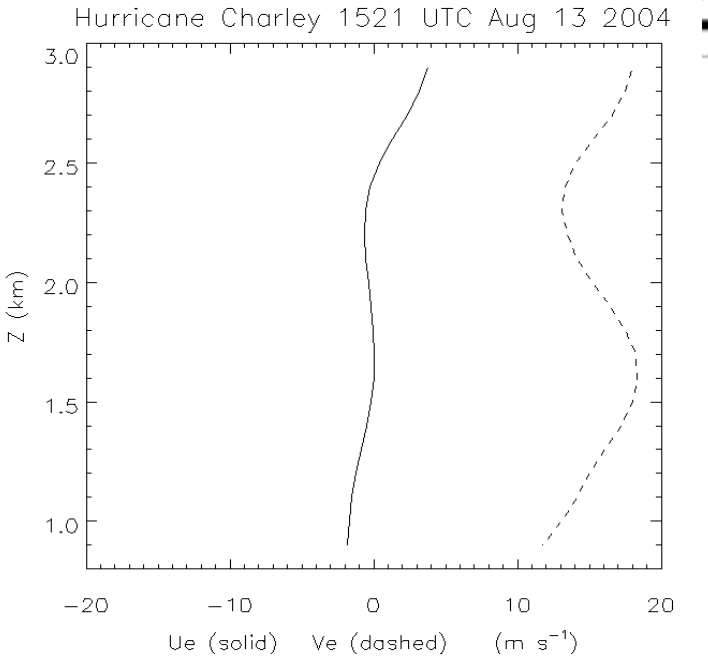

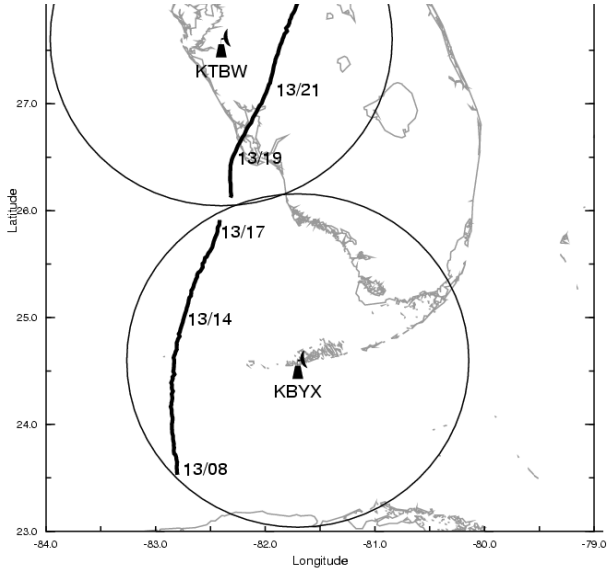

Cat.	Maximum Sustained Wind Speed m/s	Minimum Surface Pressure mb
1	33-42	>980
2	43-49	979-965
3	50-58	964-945
4	59-69	944-920
5	>70	<920

Vorticity Regime Transition

GBVTD Retrieved (Lee and Bell 2007)

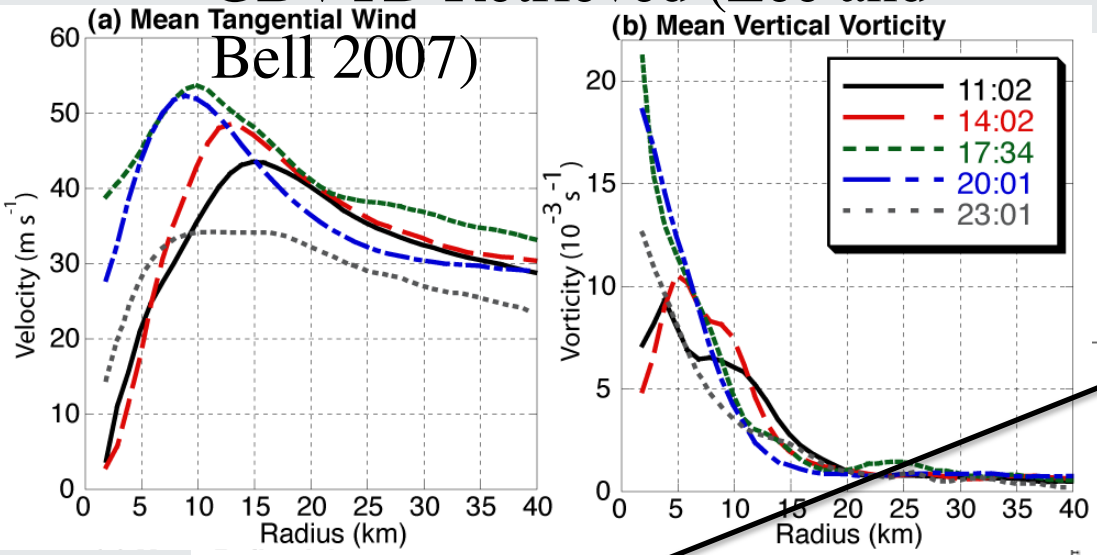

Simulation

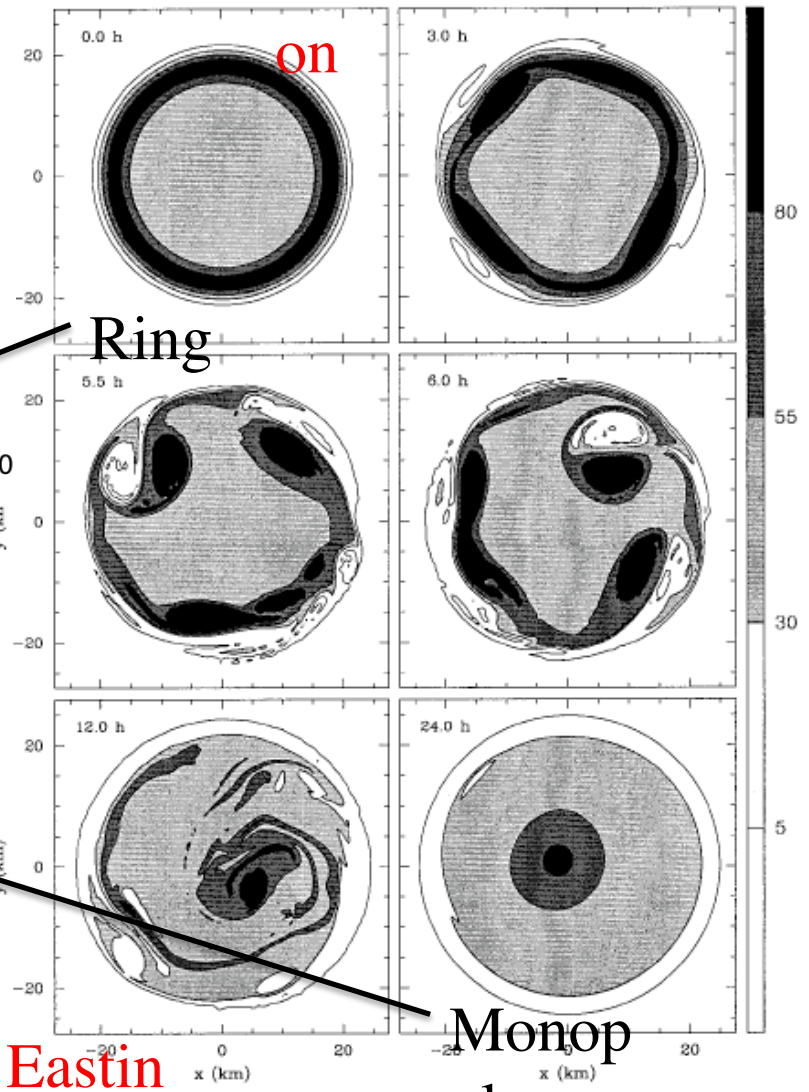

Ring

Insitu Aircraft Obs.

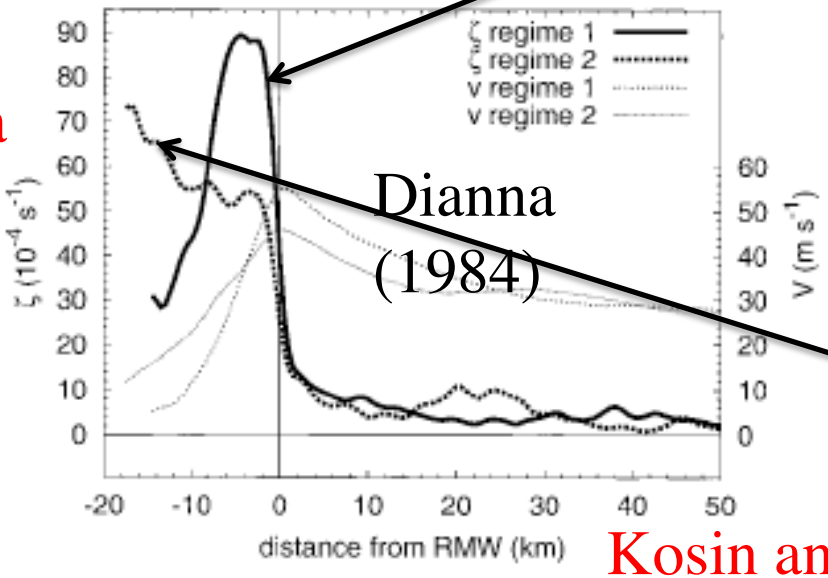

Dianna (1984)

Monopole

Kosin and Eastin (2002)

VORTRAC

Vortex Objective Radar Tracking and Circulation

- Provide time series of central pressure and RMW of landfalling TC from coastal WSR-88D data
- Integrate algorithm modules into a user-friendly environment (GUI)
- Semi-automatic operation with confidence level assigned to each estimation

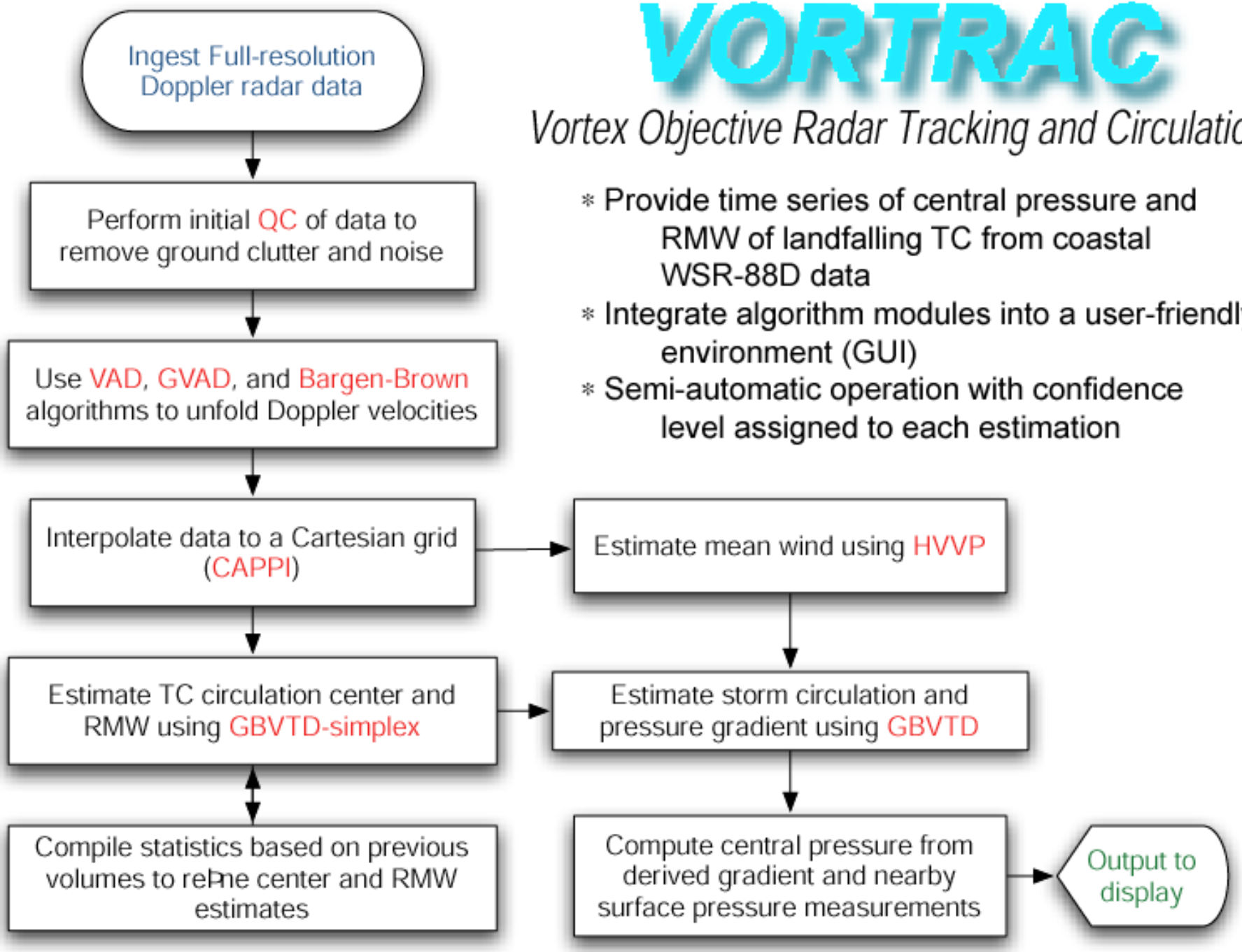

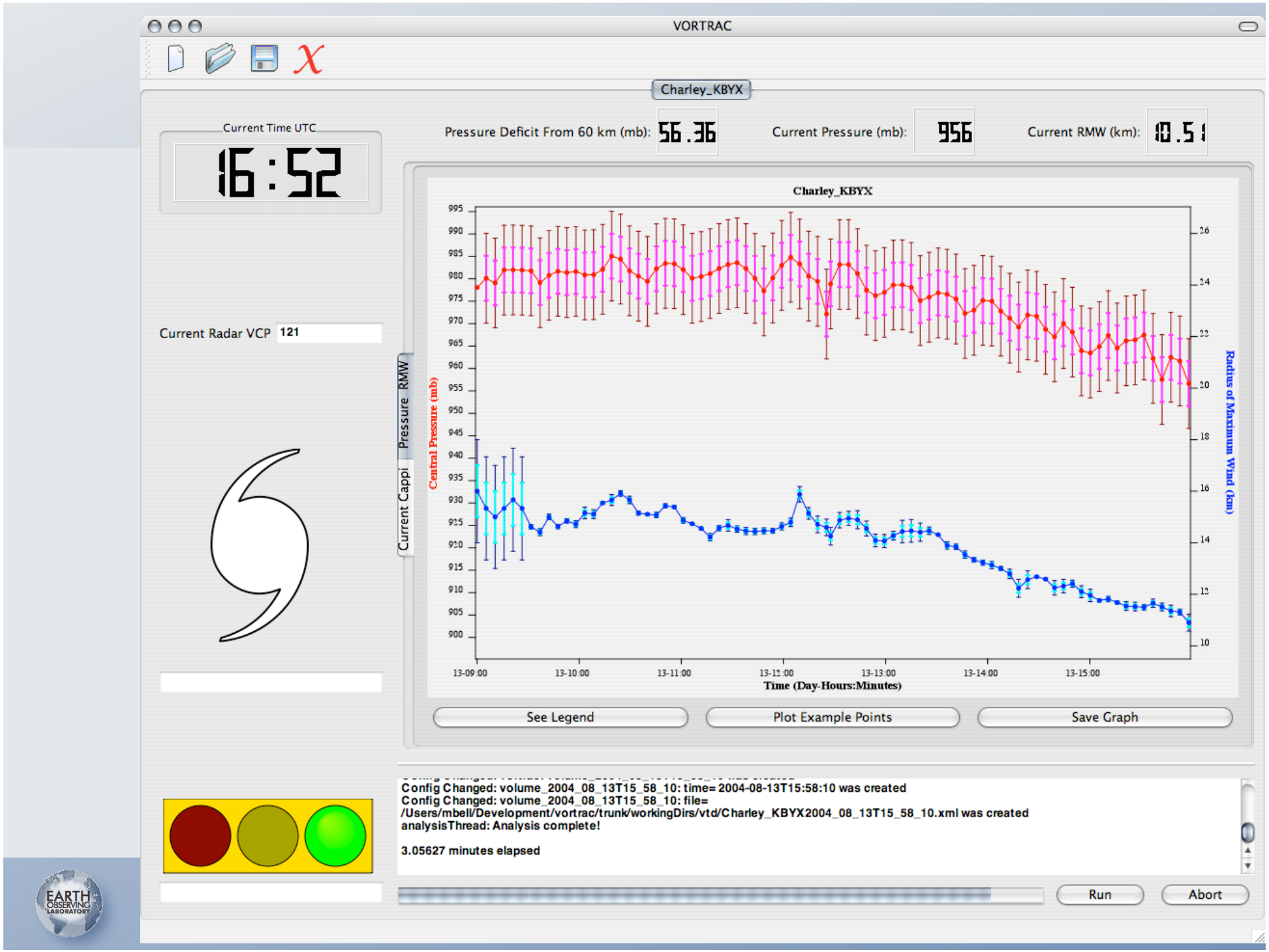
VORTRAC
Charley_KBYX
Current Time UTC
16:52
Pressure Deficit From 60 km (mb):
56.36
Current Pressure (mb):
956
Current RMW (km):
10.51
Current Radar VCP
121
Pressure
RMW
Current Cappi
Charley_KBYX
Central Pressure (mb)
Radius of Maximum Wind (km)
Time (Day-Hours:Minutes)
13-09:00
13-10:00
13-11:00
13-12:00
13-13:00
13-14:00
13-15:00
See Legend
Plot Example Points
Save Graph
Config Changed: volume_2004_08_13T15_58_10: time= 2004-08-13T15:58:10 was created
Config Changed: volume_2004_08_13T15_58_10: file=
/Users/mbell/Development/vortrac/trunk/workingDirs/vtd/Charley_KBYX2004_08_13T15_58_10.xml was created
analysisThread: Analysis complete!
3.05627 minutes elapsed
Run
Abort
EARTH OBSERVING LABORATORY

Hurricane Humberto (2007)

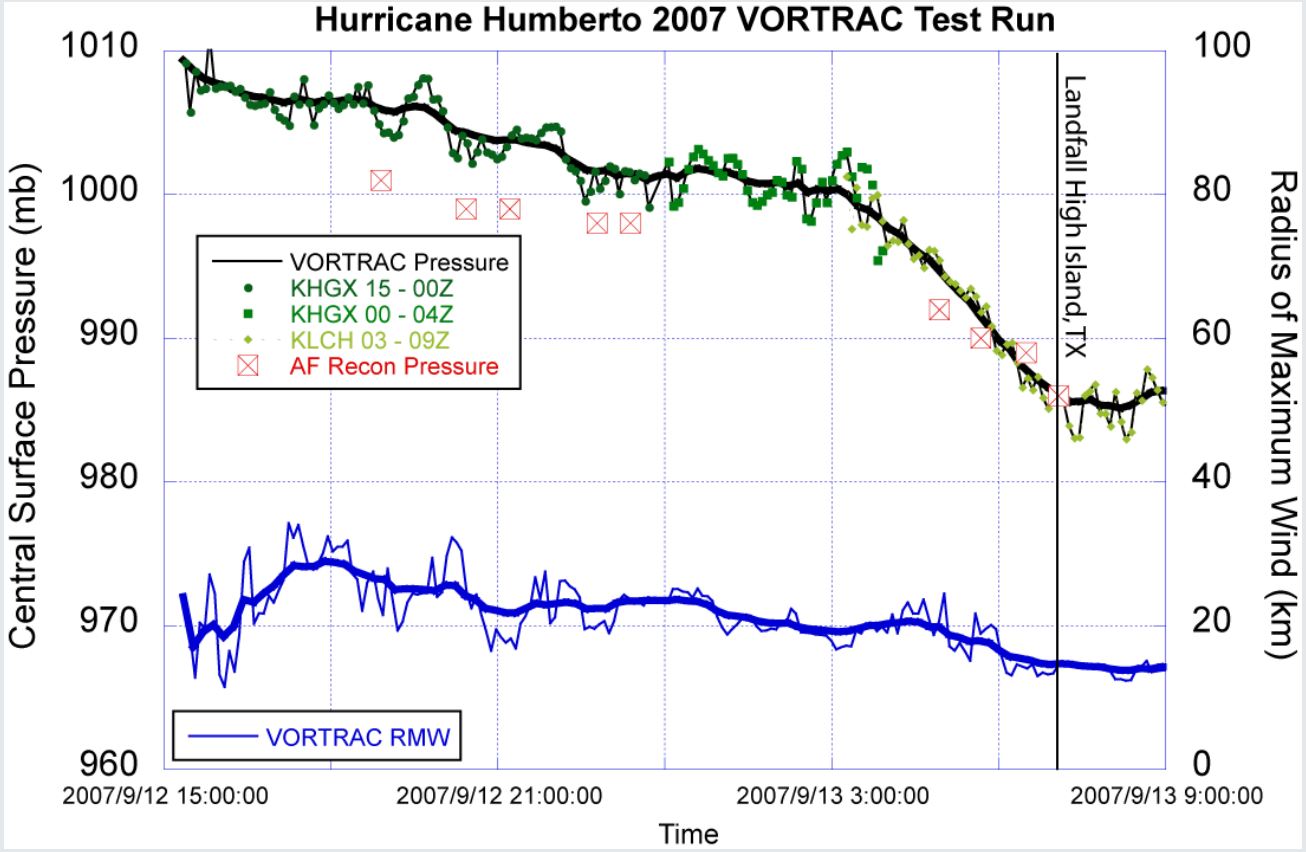

- Rapidly Intensified from TD to Hurricane in 16 hours before landfall, accompanied by a contraction of the eyewall
- VORTRAC captured this rapid intensification, agreeing well with USAF recon dropsonde measurements

VORTRAC Outside of US

- Central Weather Bureau – Taiwan
- Typhoon Monitoring and Warning System (30 June 2010) – China
  - Retrieved 3D winds
  - Environment wind
  - Typhoon center
  - 1 hr and 3 hrs QPE/QPF
  - Wind radii diagnosis
  - Applied in Typhoon 1003, 1010, and 1013
  - 34 kts and 50 kts wind radii

Airborne Phased Array Radar

- Aging ELDORA, community needs for higher spatial resolution and dual-Pol capability, emerging phased array radar technology
- Community survey in 2006
- Four C-band active element scanning array (AESA) conformal antennas
  - I
  - 2
    c
  - I

- American Recovery and Reinvestment Act (ARRA) funding to assess risks for AESA development (collaborated with MIT Lincoln Lab)
- Phased approach: 2-D array -> sub-array -> single array -> 3 additional array faces
- Potential future collaborators: MIT/LL, CSU, Ball Aerospace, NPS/CIRPAS, UMASS, OU

NSI

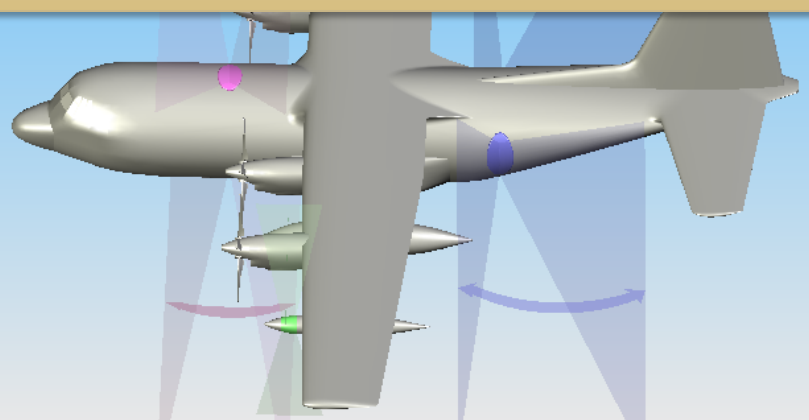

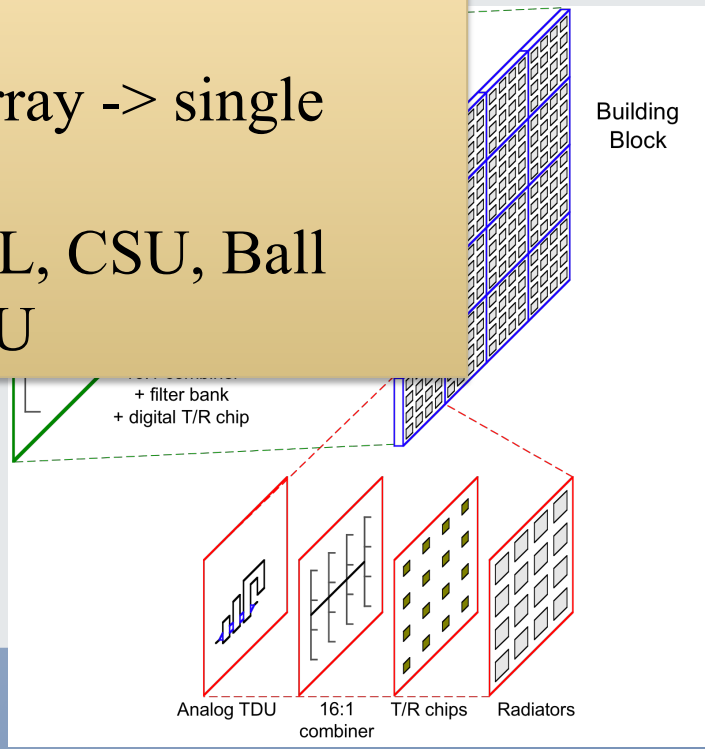

The Future

- Leave it to Frank!
- Happy 60th Birthday, Frank.